

AD-775 590

TARGET-GENERATED RANGE ERRORS

David C. Cross, et al

Naval Research Laboratory
Washington, D. C.

January 1974

DISTRIBUTED BY:

NTIS

National Technical Information Service
U. S. DEPARTMENT OF COMMERCE
5285 Port Royal Road, Springfield Va. 22151

UNCLASSIFIED

SECURITY CLASSIFICATION OF THIS PAGE(When Data Entered)

8. Projects WF-099-05-020,
UR-021-03-05, and RF-12-151-403-4018

20.

(Continued abstract)

target, scintillation is reduced completely and the target range is always confined within the target's physical extent. The range location of the target can be a "center-of-gravity" or some particular point of interest on the target, depending on how the data is processed. Since a practical system cannot resolve all complex targets, the case of partial resolution is also investigated to determine range error as a function of resolution from fully unresolved to fully resolved.

CONTENTS

Abstract	iv
INTRODUCTION	1
BASIC THEORY FOR THE UNRESOLVED TARGET (NARROW-BAND) CASE	2
Spectrum of a Time Shifted RF Pulse (Point Source Target)	3
Geometry of Two-Element Target	4
Spectrum of Two-Element Target Return	6
N-Element Complex Target	11
ANALYSIS OF RANGE ERROR FOR THE PARTIALLY AND FULLY-RESOLVED (MEDIUM AND WIDEBAND) CASE	17
EXPERIMENTAL RESULTS	18
CONCLUSIONS	21
ACKNOWLEDGMENT	23
REFERENCES	24

ABSTRACT

> Radar range tracking systems employing a narrow RF bandwidth are subject to range scintillation errors which are generated by complex targets, including multipath propagation. The errors can be many times the actual target extent. In the narrow-band case, the errors are of the same form as angle scintillation. This similarity allows the general rules applying to angle scintillation to be applied to estimate range errors for complex targets. As bandwidth is increased, range scintillation is reduced. When bandwidth is sufficient to resolve the individual parts of the target, scintillation is reduced completely and the target range is always confined within the target's physical extent. The range location of the target can be a "center-of-gravity" or some particular point of interest on the target, depending on how the data is processed. Since a practical system cannot resolve all complex targets, the case of partial resolution is also investigated to determine range error as a function of resolution from fully unresolved to fully resolved.

TARGET-GENERATED RANGE ERRORS

INTRODUCTION

Distributed complex targets such as aircraft cause scintillation in the range coordinate of a radar similar to radar target angle scintillation or glint. This scintillation causes significant errors in conventional tracking radar and is also a basic limitation to multi-lateration techniques dependent on range measurements for 3-D target location whether using pulsed or FM-CW signals. There are several situations, including multipath propagation where various degrees of resolution of the target may occur from the fully unresolved case to a fully resolved. It is the purpose of this report to relate the performance of a range tracker to the characteristics of the target which affect range estimation for the fully unresolved to fully resolved case, including the partially resolved case.

Previous work in the area of target angle scintillation caused by distributed complex targets such as aircraft has developed interest in extending the theories associated with angle scintillation to include target range scintillation [1,2,3]. Experimental data on simulated targets indicate that range scintillation is similar in nature to angle scintillation. In order to develop the theory of range scintillation and verify the results with empirical evidence, a study was undertaken to analyze range errors observed in pulse-modulated radar. The study included both analog and computer simulations. Although this report is primarily centered on pulse-modulated systems, previous work indicates these errors are observed in other range measuring systems - such as FM-CW ranging sets [4]. As shown for the narrow-band case, the range scintillation is an erroneous delay of the modulating function regardless of the type of modulations such as FM, pulse, etc.

In a basic radar ranging system a measurement is made of the time lag between the time the radar waveform is broadcast and the time the target echo is received. This time lag is directly proportional to range. In a practical pulse-modulated system the pulse length is finite; therefore, to measure the time of arrival of the echo, a reference point on the pulse must be established. Typically, the reference point is either the leading edge or "center of gravity" of the video return. If the target distorts the transmitted pulse then the reference point can move and indicate an erroneous range. Thus, target generated range errors are those errors caused by a shifting of the reference point in the return. The nature of these shifts and the mechanisms which cause them are the subjects of this report.

BASIC THEORY FOR THE UNRESOLVED TARGET (NARROW-BAND) CASE

The assumption underlying most range tracking systems is that the return is a time delayed replica of the transmitted waveform differing only in amplitude. The amplitude being a function of the target cross-section and the two-way propagation loss. Given this assumption, the reference point on the return may be defined in terms of the transmitted signal. A common reference is the "center-of-gravity" of the return envelope.

The "center-of-gravity" tracker utilizes the envelope of the radar return and a variable delay range gate. The gate is divided into two halves, the first half called the early gate, the second called the late gate. The range gate is positioned about the return waveform (either manually or by other acquisition methods) and the error detector integrates the portion of the return falling in each gate. In the closed-loop tracking mode, if the areas are not equal, the tracker repositions the gates in an effort to equalize the area in each gate. This may be expressed mathematically as follows [3]:

$$\epsilon = \int_{\tau-t_g}^{\tau} f(t)dt - \int_{\tau}^{\tau+t_g} f(t)dt \quad (1)$$

where

ϵ is the error signal

$f(t)$ is the detected waveform

τ is the center of the gate

t_g is the width of the early and late gate

In the closed-loop mode, $\epsilon = 0$, therefore:

$$\int_{\tau-t_g}^{\tau} f(t)dt = \int_{\tau}^{\tau+t_g} f(t)dt \quad (2)$$

The reference point is then taken as the time, τ , which splits the area under the detected envelope into two equal parts. Unfortunately, when the target is not a point source, slight changes in aspect can cause drastic changes in τ .

These large changes in τ arise from the fact that the typical radar target is a complex object composed of many reflecting surfaces. For simplicity, a complex target may be viewed as a collection of n point source reflectors distributed in range, each having an independent amplitude. The target return is then the vector sum of n individual signals, which tend to reinforce or cancel each other, depending on their relative phase at the time of detection. This relative phase is determined by the range of each individual reflector.

The problem of concern is what happens to the distribution of area under $f(t)$, the detected waveform, as these reflectors change relative amplitude and phase. The first case to be considered is the narrow-band case. In a pulse-modulated radar, the use of the term narrow-band implies a pulse which is long compared to the target length. A more precise definition of this case will be given later. A spectral analysis of the target return is used to explain and quantify the target-generated range errors in the narrow-band case. First, the spectrum of a point source target is examined. The properties of the spectrum associated with the range (time delay) of the target are discussed. Next, a two-element target is introduced. It is shown that under the proper conditions the two elements can generate false range information which can not be distinguished from true target range, as discussed for a point source (one-element) target.

Spectrum of a Time Shifted RF Pulse (Point Source Target)

Let the transmitted signal, $f(t)$, be defined by:

$$f(t) = m(t)e^{j\omega_c t} \quad (3)$$

where

$m(t)$ is the modulating waveform

ω_c is the RF carrier frequency.

If the Fourier transform of $m(t)$ is given as $M(\omega)$, then the Fourier transform of $f(t)$, $F(\omega)$, is:

$$F[f(t)] = F(\omega) = M(\omega - \omega_c) \quad (4)$$

The question of interest is how is the spectrum modified when the time function is shifted or delayed in the time domain. This is the case for the point source target. The Fourier transform of $f(t-t_0)$ is:

$$F [f(t-t_0)] = F(\omega) e^{-j\omega t_0} = M(\omega-\omega_c) e^{-j\omega t_0}$$

where t_0 is the time shift. This may be expressed as

$$F [f(t-t_0)] = M(\omega-\omega_c) e^{-j\phi_s(\omega)} \quad (5)$$

The expression in Equation (5) implies that when a waveform is time shifted by t_0 , the round trip time delay, each frequency component is shifted in phase by an amount ωt_0 , designated $\phi_s(\omega)$, (i.e., a phase which is a linear function of frequency is added to each spectral component). Amplitude change due to the target cross-section and propagation losses are omitted since they are normalized by an AGC function.

Since a time shift implies a linear phase shift versus frequency throughout the spectrum, a linear phase characteristic will appear in the Fourier transform of any undistorted time-shifted signal. The time shift, t_0 , appears in the phase versus frequency portion of the transform as the coefficient of ω . The two-target case is examined next to demonstrate how false range information can be generated by the addition of a second reflector.

Geometry of Two-Element Target

Figure 1 shows a two-element target having relative amplitude, b , and relative phase, ϕ_R . Relative amplitude, b , is the ratio of the amplitude of the nearer reflector to the amplitude of the farther reflector. The relative phase, ϕ_R , is the two-way radial target length - measured along the boresight axis at the carrier frequency - expressed in radians and is defined from the geometry as follows:

$$\phi_R = \frac{2\omega_c}{c} L \sin \psi$$

where

ω_c is the carrier frequency

L is the target length

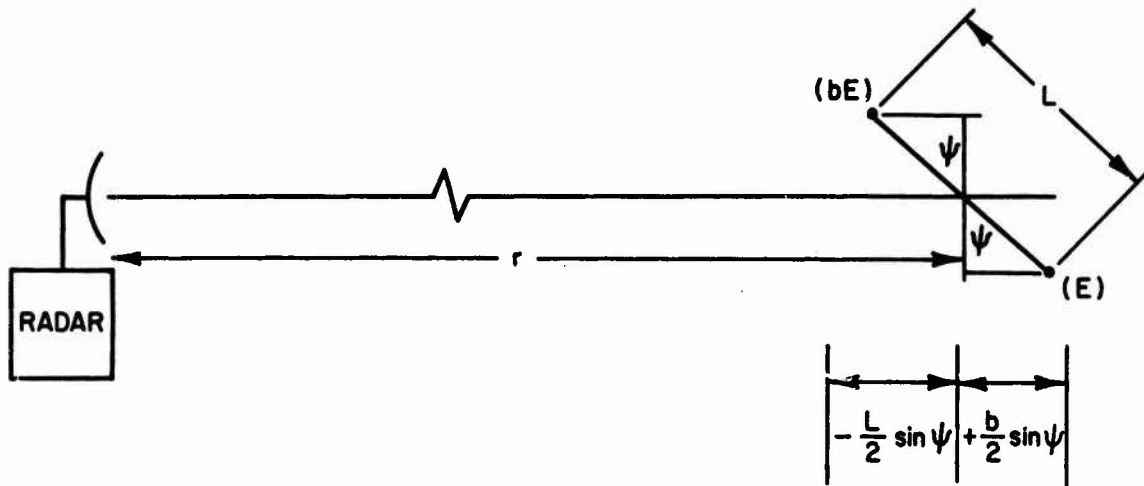


Fig. 1 - Two-element target geometry

c is the speed of light

ψ is the aspect angle measured from a normal to the boresight axis through the target midpoint.

Spectrum of Two-Element Target Return

By using the target depicted in Fig. 1, a coordinate system measuring time from the midpoint of the target, and a modulation waveform $m(t)$ with Fourier transform, $M(\omega)$, the return waveform $f(t)$, can be written as follows:

$$f(t) = bm \left(t + \frac{t_0}{2} \right) e^{j\omega_c \left(t + \frac{t_0}{2} \right)} + m \left(t - \frac{t_0}{2} \right) e^{j\omega_c \left(t - \frac{t_0}{2} \right)} \quad (6)$$

where the two way time delay of the farther element relative to the near element is

$$t_0 = \frac{2L \sin \psi}{c}, \text{ as shown in Fig. 1.}$$

Using the time and frequency shifting properties of Fourier transforms, the transform of $f(t)$ is [5]

$$F(f(t)) = F(\omega) = M(\omega - \omega_c) \left\{ e^{-j\omega \frac{t_0}{2}} + b e^{+j\omega \frac{t_0}{2}} \right\}$$

Simplifying,

$$F(f(t)) = A(\omega) M(\omega - \omega_c) e^{-j\phi_s(\omega)} \quad (7)$$

where

$$A(\omega) = \sqrt{1 + b^2 + 2b \cos \omega t_0}$$

and

$$\phi_s(\omega) = \tan^{-1} \left\{ \frac{(1-b) \sin \omega \frac{t_0}{2}}{(1+b) \cos \omega \frac{t_0}{2}} \right\} \quad (8)$$

Thus, $F(\omega)$ is given by the product of the transform of the modulating waveform, $M(\omega - \omega_c)$, and amplitude factor $A(\omega)$, with a phase, $\phi_s(\omega)$. The amplitude and phase characteristics are a function of the target only. If the amplitude were constant and the phase were linear with frequency, the inverse transform would be a time-shifted undisturbed version of the modulating waveform. The magnitude of the time shift is given by the slope of phase versus frequency, as shown later.

Although the amplitude is not constant and phase is not linear for the two-element target when observed over a wide frequency region, a narrow-band radar will observe only a small segment of the amplitude and phase functions. Within this small segment the amplitude, $A(\omega)$, will be essentially constant and phase versus frequency essentially linear. Consequently, the radar sees what appears like the echo from a point source. This can be verified by performing a Taylor series expression of the phase function $\phi_s(\omega)$ about the carrier frequency ω_c . The Taylor series gives:

$$\phi_s(\omega) = \phi_s(\omega_c) + \phi_s'(\omega_c) (\omega - \omega_c) + \frac{\phi_s''(\omega_c)}{2!} (\omega - \omega_c)^2 + \dots$$

With the above assumption that $\phi_s(\omega)$ is essentially linear over the region of interest, the higher order terms of the series may be omitted leaving:

$$\phi_s(\omega) \approx \phi_s(\omega_c) + \phi_s'(\omega_c) (\omega - \omega_c).$$

Also, since $A(\omega)$ is essentially constant, it may be replaced with a constant, $A(\omega_c)$, and Equation (7) may be rewritten as:

$$F(\omega) \approx A(\omega_c) M(\omega - \omega_c) e^{-j \{ \phi_s(\omega_c) + \phi_s'(\omega_c) (\omega - \omega_c) \}}$$

or

$$F(\omega) \approx A(\omega_c) e^{j [\omega_c \phi_s'(\omega_c) - \phi_s(\omega_c)]} M(\omega - \omega_c) e^{-j \omega \phi_s'(\omega_c)} \quad (9)$$

Taking the inverse transform

$$\begin{aligned} \mathcal{F}^{-1} \{ F(\omega) \} &= A(\omega_c) e^{j [\omega_c \phi_s'(\omega_c) - \phi_s(\omega_c)]} m(t - \phi_s'(\omega_c)) e^{+j \omega_c [t - \phi_s'(\omega_c)]} \\ &= A(\omega_c) m(t - \phi_s'(\omega_c)) e^{+j [\omega_c t - \phi_s(\omega_c)]} \end{aligned} \quad (10)$$

Thus, the return in the narrow-band case appears as a time shifted version of the transmitted signal attenuated by a factor, $A(\omega_c)$, with a phase shift, $-\phi_s(\omega_c)$, added to the carrier.

As seen from Equation (10), the amount of time shift is given by the derivative of $\phi_s(\omega)$ evaluated at ω_c . It is interesting to note that the carrier phase shift is not sensed by a radar using the range tracking techniques considered in this report since only the detected signal is utilized; however, this phase shift will cause errors in coherent phase tracking systems. It is the slope of phase versus frequency which causes the errors considered here in the narrow-band case.

The "narrow-band" condition occurs when the radar pulse length is long compared to target length (expressed by t_0), which represents essentially a completely unresolved complex target. This is demonstrated in Fig. 2 for a specific combination of target length relative amplitude and pulse length. A relatively long Gaussian pulse shape was assumed for the modulation waveform. The resulting Gaussian-shaped spectrum is, therefore, narrow, as seen in the plots for two different carrier frequencies in Fig. 2.

The carrier frequencies were chosen for the extreme cases so that at one carrier frequency the returns from each reflector add, and for the other the returns cancel. The upper curve is a plot of $\phi_s(\omega)$ generated by the target. The lower curves are the transmitted spectra, $M(\omega - \omega_c)$, using the two different carriers. The interesting point to note about this figure is that the slope of $\phi_s(\omega)$ is essentially constant over the extent of each spectrum, but of considerably different magnitude for each spectrum. The different slopes indicate correspondingly different target ranges even though the two-element target has not moved. The magnitude of this apparent motion in range can be large compared to the target span, as shown later. The magnitude function, $A(\omega)$, (not shown) is also constant over the narrow spectra. The constant slope and magnitude are the exact properties discussed earlier, which are found in the spectrum of a time shifted point source return.

In this illustration, the carrier frequency ω_c was changed to alter the relative phase of the returns from each element of the target in order to simplify the illustration. However, in practice, the carrier is held constant and slight changes in aspect angle ψ (Fig. 1) would result in the change of relative phase. A change in ψ will alter the target length, t_0 , but at RF frequencies the change could be quite small, on the order of 0.5 pico seconds, a quarter

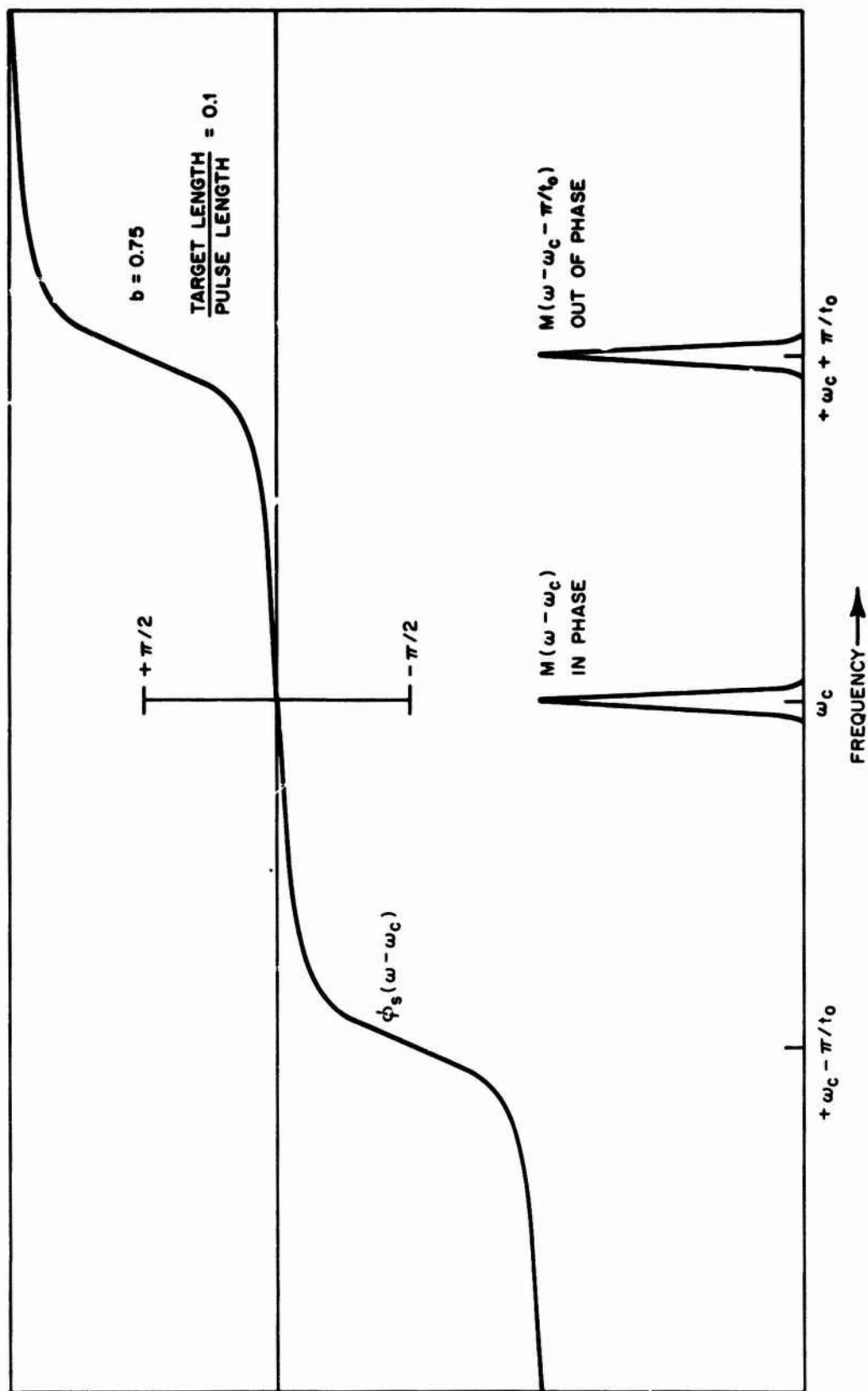


Fig. 2 - Target phase characteristic over signal bandwidth

wavelength, or a fraction of an inch at 10 GHz. This change is an insignificant portion of a target span for targets of a few yards length, yet the resultant change in slope of $\phi_s(\omega)$ will give an apparent range movement of several target spans.

From this discussion, it can be seen that in the narrow-band case the target generated contributions to the spectrum are essentially the same as the time shift properties discussed for the point source target. The magnitude of the time shift, Δt , associated with a given relative phase, $\omega_c t_0$, is found by evaluating the derivative of $\phi_s(\omega)$ at ω_c .

The derivative is given by:

$$\phi_s'(\omega) = t_0/2 \frac{1-b^2}{1+b^2+2b \cos(\omega t_0)}$$

$$\therefore \Delta t = \phi_s'(\omega_c) = t_0/2 \frac{1-b^2}{1+b^2+2b \cos(\omega_c t_0)} \quad (11)$$

where

b is the relative amplitude

ω_c is the carrier frequency

t_0 is the target length expressed in time

$\omega_c t_0$ is the relative phase of the two returns.

For the in-phase condition,

$$\omega_c t_0 = n(2\pi)$$

$$\Delta t = \frac{1-b}{1+b} t_0/2$$

and, for the out-of-phase case,

$$\omega_c t_0 = n(2\pi) + \pi$$

$$\Delta t = \frac{1+b}{1-b} t_0/2$$

Figure 3 is a plot of the detected envelope (using linear detection) of the target described in Fig. 1, with relative amplitude equal to 0.9 and radiated with a Gaussian pulse one hundred times the target length. For the assumed target, this pulse length is sufficiently long to approximate the linear phase and constant amplitude characteristics needed for undistorted time translation.

The envelope formed by vectorially adding the return from each element in the time domain and using linear detection has been plotted for the in-phase, ($\omega_{ct0} = 2n\pi$), and out-of-phase, ($\omega_{ct0} = 2n\pi + \pi$), case with an AGC operation to remove the amplitude difference due to the cancellation in the out-of-phase case. The only difference in these waveforms is a shift in time in the direction of the stronger target for the out-of-phase condition. In this example, the time shift is equal to 9.5 times the target length. From this illustration, it can be seen that no matter how the waveform is processed, this time shift can not be distinguished from real target range movement. In reality, no range movement, but only a slight change in aspect angle, is required to produce such drastic range errors.

Figure 4 shows a continuous plot of $\phi_s'(\omega)$ versus relative phase for various relative amplitudes of 2, 1.414, 0.5, 0.707, and 0.9. As illustrated, the range errors can indicate target range is outside the physical extent of the target. Thus, in the narrow-band case, the area under the video curve is shifted in time and an early-late gate tracker will simply follow this shift. The leading edge is also shifted so a leading-edge tracker can not discriminate against these errors. Similarly, an FM-CW range-measuring system, which measures range by the phase shift of the received FM modulation, will observe an erroneous time shift of the modulation.

This error, as a function of spacing or relative phase between reflectors, is essentially the same as in the angle-scintillation case [1,2,3]. The difference is that the range error is proportional to the range separation of the sources while the angle error is proportional to the angular separation of the two sources. This basic result also holds for a n-element target, which is discussed below.

N-Element Complex Target

For a target composed of n reflectors illuminated with a narrow-band waveform, the range error can be obtained in the same manner as for the two-element target. The geometry for the n-element target

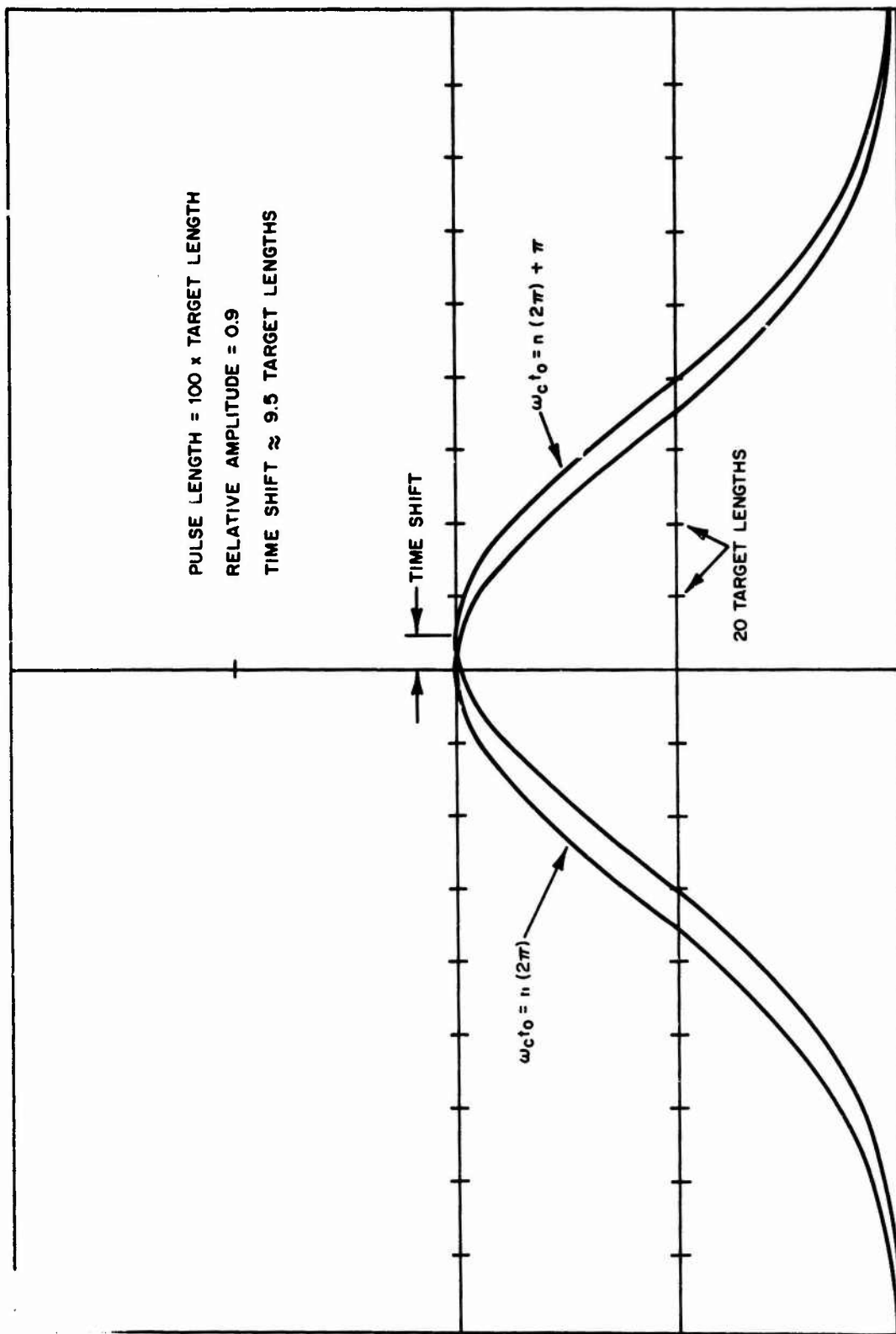


Fig. 3 - Narrow-band time translation

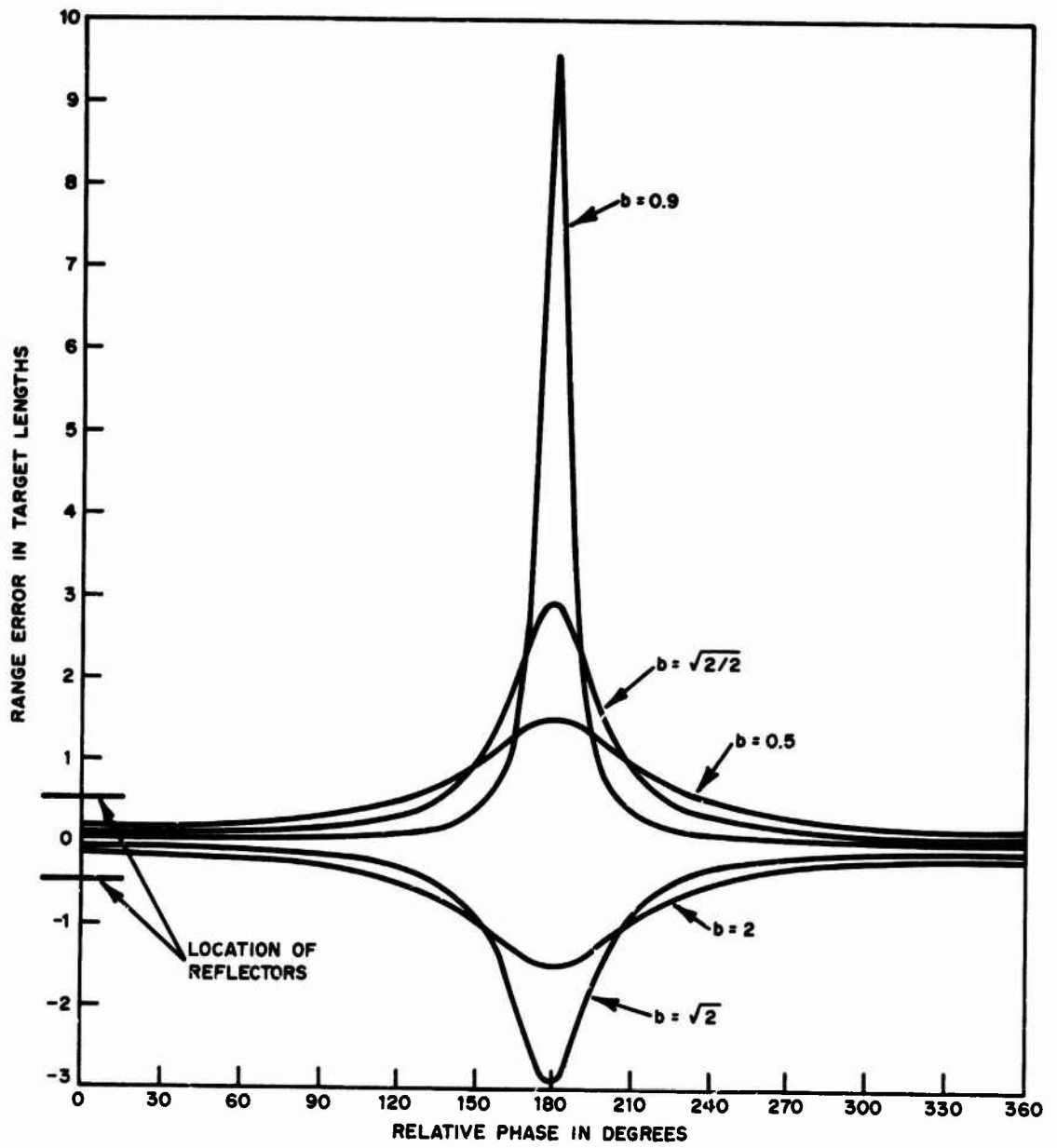


Fig. 4 - Range error versus relative phase (two-element target)

is shown in Fig. 5. The return waveform, $f_n(t)$, is then given by:

$$f_n(t) = \sum_{i=1}^n A_i m(t-t_i) e^{j\omega_c(t-t_i)} \quad (12)$$

where

$$t_i = \frac{2L_i \sin \psi_i}{c}$$

L_i is the two-way extent of the i^{th} element measured from the target midpoint

ψ_i is the aspect angle of the i^{th} element measured normal to the radar line-of-sight

c is the speed of light.

The Fourier transform of $f_n(t)$, $F_n(\omega)$, is:

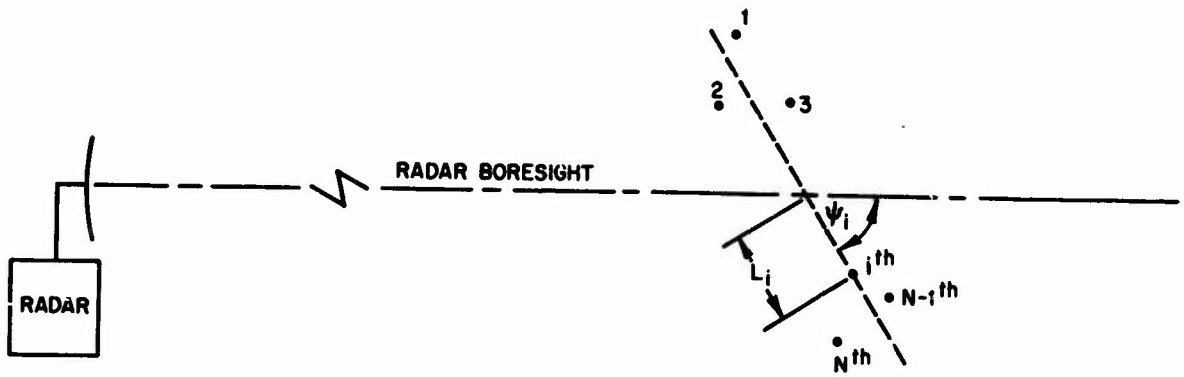
$$F_n(\omega) = M(\omega-\omega_c) \sum_{i=1}^n A_i e^{-j\omega t_i} = A_n(\omega) M(\omega-\omega_c) e^{j\phi_n(\omega)} \quad (13)$$

where

$$A_n(\omega) = \sqrt{\left[\sum_{i=1}^n A_i \sin(\omega t_i) \right]^2 + \left[\sum_{i=1}^n A_i \cos(\omega t_i) \right]^2}$$

$$= \sqrt{\sum_{i=1}^n \sum_{j=1}^n A_i A_j \cos \left[\frac{\omega}{c} (t_i - t_j) \right]}$$

$$\phi_n(\omega) = \tan^{-1} \left\{ \frac{\sum_{i=1}^n A_i \sin(\omega t_i)}{\sum_{i=1}^n A_i \cos(\omega t_i)} \right\}$$



n - ELEMENT GEOMETRY

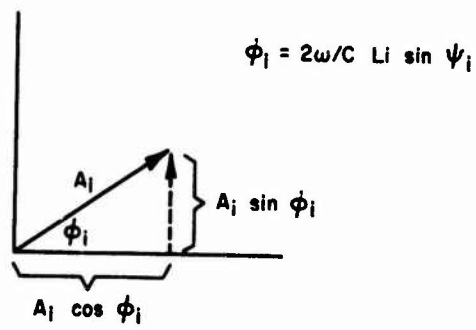


Fig. 5 - Real and imaginary components of i^{th} element

The slope of $\phi_n(\omega)$, the range error, is then:

$$\phi_n'(\omega) = \frac{\sum_{i=1}^n \sum_{j=1}^n A_i A_j \frac{2L_i \sin \psi_i}{c} \cos \left[\frac{\omega}{c}(t_i - t_j) \right]}{\sum_{i=1}^n \sum_{j=1}^n A_i A_j \cos \left[\frac{\omega}{c}(t_i - t_j) \right]} \quad (14)$$

This function is identical in form to that derived for angle scintillation by Howard [2].

$$\gamma = \frac{\sum_{i=1}^n \sum_{j=1}^n A_i A_j \theta_i \cos \left[\frac{\omega}{c}(t_i - t_j) \right]}{\sum_{i=1}^n \sum_{j=1}^n A_i A_j \cos \left[\frac{\omega}{c}(t_i - t_j) \right]}$$

where

γ is the target-generated angle error

A_i, A_j are the amplitude of the i^{th} and j^{th} reflectors respectively

θ_i is the angular distance off boresight of the i^{th} reflector.

Consequently, the general rules relating target configuration to angle scintillation will hold for range scintillation. In particular, the expression relating total rms open-loop angle scintillation error with slow AGC derived by Lewis and Howard [1] will also hold for range tracking errors. For targets composed of many reflecting surfaces, the angle scintillation is given by:

$$\sigma_{\text{ANG}}^2 = \theta_0^2 + \frac{1}{2} R_0^2$$

where

σ_{ANG} is the rms target-generated angle noise

θ_0 is the lag angle of the radar boresight with respect to the target center, and

R_0 is the radius of gyration of the reflecting area of the target along the angle-tracking axis.

Similarly, range scintillation for the open-loop case will be given by:

$$\sigma_{\text{RNG}}^2 = E_R^2 + \frac{1}{T} R_O^2, \text{ for the narrow-band case,}$$

where

σ_{RNG} is the rms target-generated range noise

E_R is the range gate lag with respect to the target center of gravity, and

R_O is the radius of gyration of the reflecting area of the target taken along the range axis.

ANALYSIS OF RANGE ERROR FOR THE PARTIALLY AND FULLY-RESOLVED (MEDIUM AND WIDEBAND) CASE

In the narrow-band case, range errors were shown to be equal to the slope of $\phi_S(\omega)$. As bandwidth is increased, the assumption that a linear phase and constant amplitude characteristics are applied to the spectrum is no longer valid. Instead, a non-linear phase characteristic, $\phi_S(\omega)$, and non-constant amplitude function, $A(\omega)$, are applied to the transmitted signal. This results in a distortion of the envelope of the return. The question of concern in evaluating the performance of an early-late gate tracker against such a target is: how is the area under this envelope redistributed along the time axis by the distortion.

Equation (7) can be rewritten in the following manner to give an insight into the area shift.

$$\begin{aligned} F(\omega) &= M(\omega - \omega_c) \left\{ e^{-j\omega t_0/2} + b e^{+j\omega t_0/2} \right\} \\ &= M(\omega - \omega_c) \left\{ \cos \omega t_0/2 - j \sin \omega t_0/2 + b \cos \omega t_0/2 + b j \sin \omega t_0/2 \right\} \\ &= M(\omega - \omega_c) \left\{ (1+b) \cos \omega t_0/2 + j(b-1) \sin \omega t_0/2 \right\} \\ &= M(\omega - \omega_c) \left\{ \frac{1+b}{2} (e^{j\omega t_0/2} + e^{-j\omega t_0/2}) + \frac{(b-1)}{2} (e^{j\omega t_0/2} - e^{-j\omega t_0/2}) \right\} \quad (15) \end{aligned}$$

$$\begin{aligned}
\therefore f(t) &= \mathcal{F}^{-1} (F(\omega)) \\
&= \frac{1+b}{2} m(t+t_0/2) e^{j\omega_c(t+t_0/2)} + \frac{1+b}{2} m(t-t_0/2) e^{j\omega_c(t-t_0/2)} \\
&\quad - \frac{1-b}{2} m(t+t_0/2) e^{j\omega_c(t+t_0/2)} + \frac{1-b}{2} m(t-t_0/2) e^{j\omega_c(t-t_0/2)}
\end{aligned} \tag{16}$$

Equation (16) states that the distortion resulting from $A(\omega)$ and $\phi_s(\omega)$ is the sum of four undistorted replicas of the transmitted signal properly weighted in amplitude and shifted in time.

This representation of the echo from the two-element target divides the received waveform into its symmetrical and asymmetrical components. The sum of the first two terms in Equation (16) is a waveform with even symmetry about the midpoint of the target. If these terms comprised the entire signal, then the signal center of area, as sensed by an early-late gate discriminator, would fall in the center of the target. However, the last two terms have odd symmetry about the midpoint. The odd symmetry upsets the balance of area and the discriminator must drive toward the stronger reflector.

The exact amount of the shift in the tracking point is not readily demonstrated analytically. The problem is to solve the closed-loop expression determining "center-of-gravity" as shown in Equation (2). A computer program was written to solve this expression for a Gaussian pulse shape. The output of this program, showing the range error as a function of bandwidth, is shown in Fig. 6. The data in Fig. 6 agree with the limit of the error in the narrow-band case for both in-phase and out-of-phase conditions. The limit in the wideband case (i.e., when the pulse is short compared to target length) converges to the position of the strongest reflector and is insensitive to relative phase. This is a logical result since a large bandwidth implies the pulses are resolved; hence, the distortion is not affected by relative phase, and the balance of the area must be inside the larger target.

EXPERIMENTAL RESULTS

Figure 7 shows an experimental setup used to measure the range errors for a fixed bandwidth and target length. An actual early-late gate range tracker was used to measure the range shifts generated by

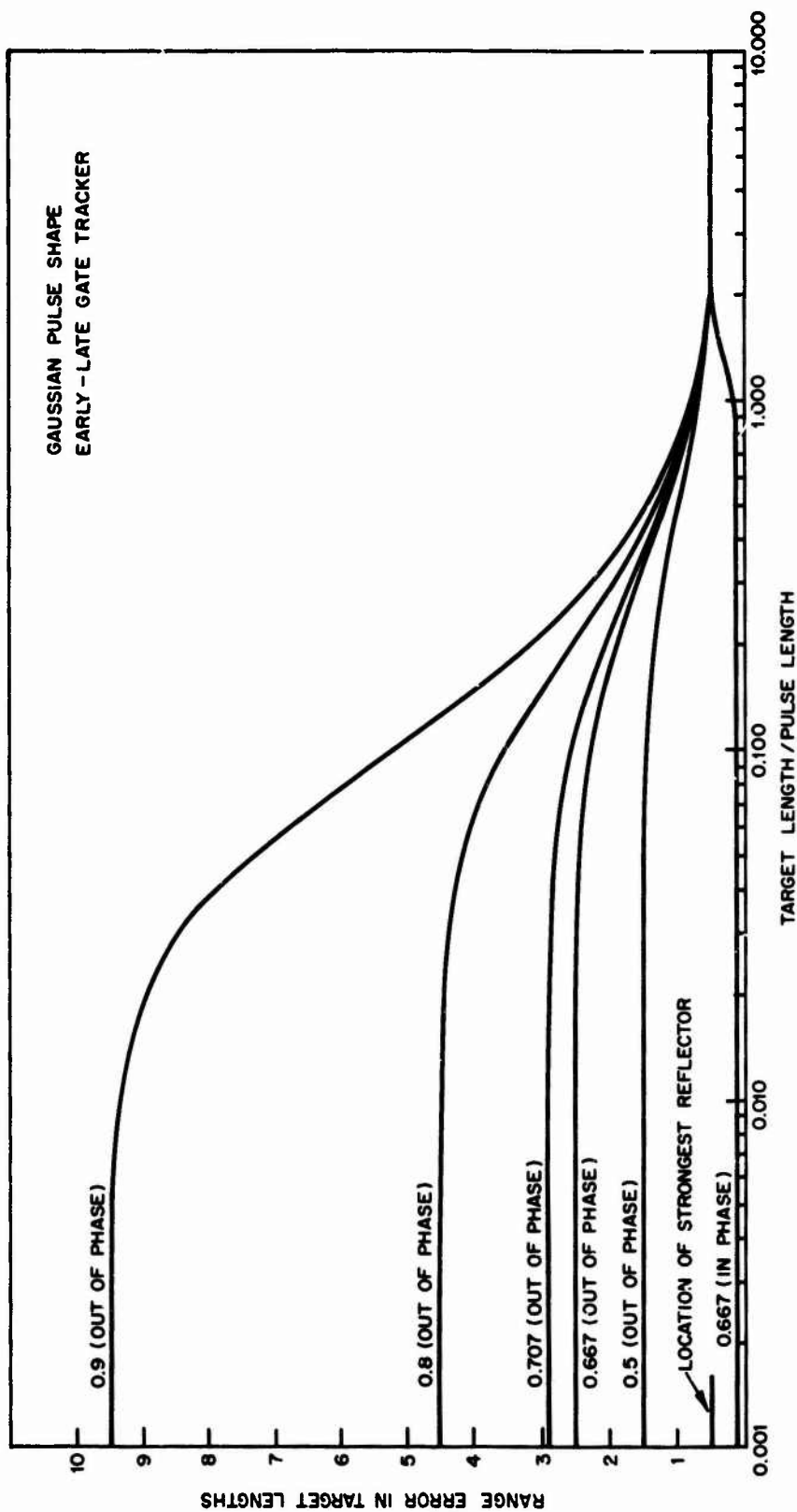


Fig. 6 - Closed loop range error versus resolution

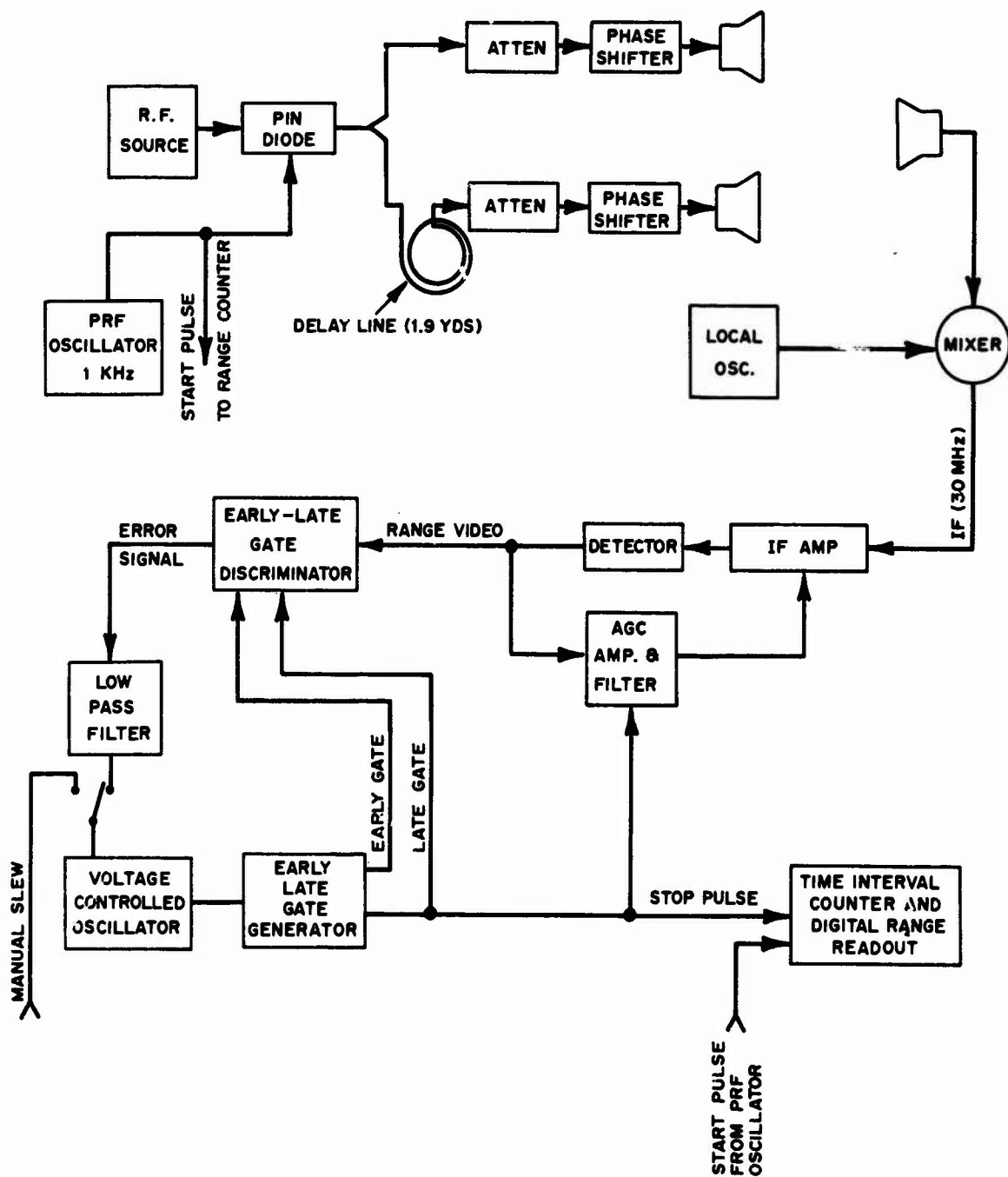


Fig. 7 - Block diagram of two-element target simulator and range tracker

a two-element target as relative phase was varied. The two targets were separated by 1.9 yards in range with a relative amplitude of approximately 0.87. Range deviation from the average range of the two-target elements (target midpoint) was measured as relative phase was varied through one complete cycle. The range deviations were expressed in target lengths and plotted as a function of relative phase. A 0.25 microsecond pulse was used as the transmitter pulse; therefore, the pulse length was approximately twenty-one times the target length. The large pulse-to-target-length ratio meets the linear phase and constant amplitude criteria for the narrow-band case. The experimental data, therefore, should agree with the slope of the phase characteristic, $\phi_s'(\omega)$, using the proper value of relative amplitude. The results of this experiment are plotted with $\phi_s'(\omega)$ in Fig. 8. As is indicated in the figure, the theory is validated by the measured data.

CONCLUSIONS

In the narrow-band case, target-generated range errors are proportional to the slope of the phase added to the transmitted spectrum by the target. The error slope is essentially constant over the frequency extent of the spectrum; therefore, the range errors are represented by an actual time shift of the return. These shifts cannot be distinguished from actual target motion by standard range processors in either FM-CW or pulse-type range trackers. Since the slope of the phase function is dependent on the relative phase of the individual reflectors, range errors are a function of relative phase. The magnitude of these errors can indicate that the range is outside the physical extent of the target. The expression for range error in the narrow-band case, given by Equation (16) for the complex target, is similar to that derived by Howard for angle scintillation. The only difference arises from the fact that range scintillation is measured in time and is directly related to the range distribution of the target, while angle scintillation is measured in the angle coordinate orthogonal to the range measurement and is directly related to the distribution of the target in the angle coordinate. Further, this similarity allows the general rules relating angle scintillation to the target distribution in the angle coordinate to be used to describe range scintillation as a function of the target distribution in the range coordinate. In particular, when tracking lag is small, range scintillation is equal to $1/\sqrt{2}$ times the radius of gyration of the reflecting area of the target taken along the range axis.

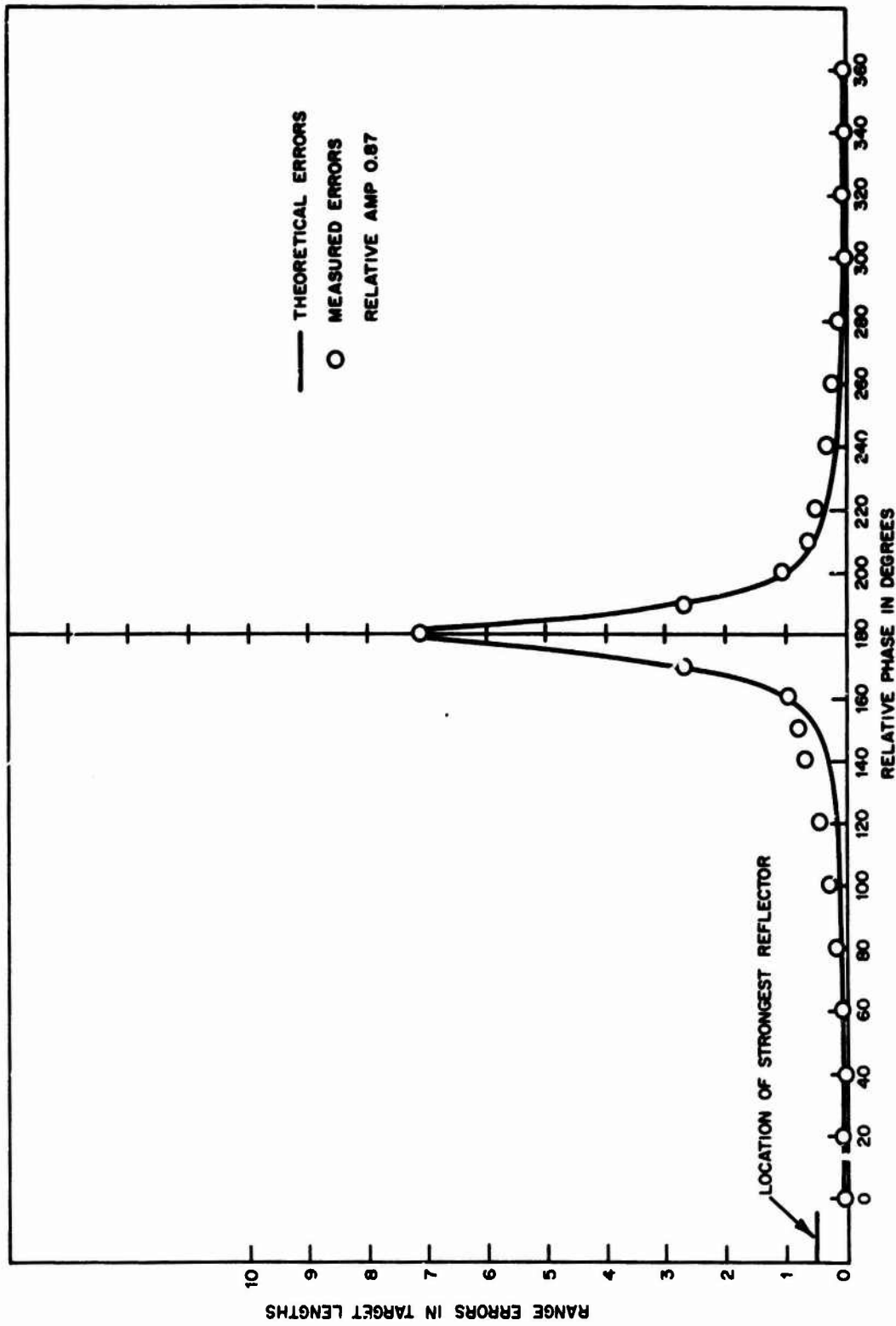


Fig. 8 - Comparison of theoretical and measured range error versus relative phase

As bandwidth is increased, range errors result more from a distortion of the range video than from a pure time translation. The exact magnitude of the errors is a function of the processing techniques, as well as the target characteristics. As more bandwidth is used to track a given target, the maximum errors are reduced from the peak errors observed in the narrow-band case. If bandwidth is increased to the point that individual reflectors are resolved, range errors are no longer sensitive to relative phase. In the resolved case, the range will always lie within the physical extent of the target. The exact range will then be a function of the tracking technique.

ACKNOWLEDGMENT

The authors thank Messrs. D. D. Howard and J. P. Barry of the Radar Division for their suggestions and guidance during the writing of this report.

REFERENCES

- [1] Lewis, B. L. and Howard, D. D., "Radar Tracking Noise in Theory and Practice," NPL Report 4830, November 1956.
- [2] Howard, D. D., "Radar Target Angular Scintillation in Tracking and Guidance Systems Based on Echo Signal Phase Front Distortion," Proc. N.E.C., Vol. 15, pp. 840-849, October 1959.
- [3] Barton, D. K. and Ward, H. R., "Handbook of Radar Measurements," Prentice Hall, Inc., Englewood Cliffs, New Jersey, Ch. 3, pp. 49-89, 1969.
- [4] King, A. M., Morrow, C. M., Myers, C. G., Moody, C. L., "Scintillation Range Noise and Related Phenomena in Water Wave Profiling with Microwave Radar," NRL Report 6641, September 1968.
- [5] Lathi, B. P., "Communication Systems," John Wiley and Sons, Inc., New York, New York, Ch. 1, pp. 73-75, 1968.